*Journal of Experimental Botany*, Vol. 72, No. 22 pp. 7984–7997, 2021
https://doi.org/10.1093/jxb/erab384 Advance Access Publication 19 August 2021

RESEARCH PAPER

# Xylem biomechanics, water storage, and density within roots and shoots of an angiosperm tree species

**Alex B. Baer, Jaycie C. Fickle, Jackeline Medina, Catherine Robles, R. Brandon Pratt and Anna L. Jacobsen***

Department of Biology, California State University, Bakersfield, CA, 93311, USA

*Correspondence: ajacobsen@csub.edu

Received 3 March 2021; Editorial decision 13 August 2021; Accepted 17 August 2021

Editor: Howard Griffiths, University of Cambridge, UK

## Abstract

**Xylem is a complex tissue that forms the bulk of tree bodies and has several functions, including to conduct water, store water and nutrients, and biomechanically support the plant body. We examined how xylem functional traits varied at different positions within 9-year-old *Populus balsamifera* subsp. *trichocarpa*. Whole trees were excavated, and xylem samples were collected at 1-m increments along the main root-to-shoot axis of six trees, from root tip to shoot tip. We examined biomechanical and water-storage traits of the xylem, including using a non-invasive imaging technique to examine water content within long, intact branches (high-resolution computed tomography; microCT). Xylem density, strength, and stiffness were greater in shoots than roots. Along the main root-to-shoot axis, xylem strength and stiffness were greatest at shoot tips, and the tissue became linearly weaker and less stiff down the plant and through the root. Roots had greater water storage with lower biomechanical support, and shoots had biomechanically stronger and stiffer xylem with lower water storage. These findings support trade-offs among xylem functions between roots and shoots. Understanding how xylem functions differ throughout tree bodies is important in understanding whole-tree functioning and how terrestrial plants endure numerous environmental challenges over decades of growth.**

**Keywords:** Black cottonwood, capacitance, HRCT, modulus of elasticity (MOE), modulus of rupture (MOR), moisture release curve, poplar, *Populus balsamifera*, *Populus trichocarpa,* strength, stiffness, water potential.

## Introduction

Trees are large-bodied perennial plants that grow long, subterranean roots and tall, aerial shoots made predominantly of a single vascular tissue, xylem, that experiences a range of localized environmental conditions across the plant organs. Trees must be well anchored and biomechanically reinforced to protect against buckling, bending, and uprooting (Putz *et al.*, 1983; van Gelder *et al.*, 2006). As well as fulfilling this function, xylem is also responsible for the transport of water under tension from roots to leaves. Stored water inside xylem is an asset for maintaining water transport by minimizing water potential declines; however, water storage requires space inside the xylem (Holbrook, 1995) that may

conflict with its biomechanical function (Pratt and Jacobsen, 2017).

The biomechanical strength of xylem protects the tree body from deformation and collapse caused by both external and self-imposed forces. Mechanical forces do not act uniformly within the complex structure of trees (Niklas, 1992; van Gelder *et al.*, 2006). The vertical orientation of a shoot requires that xylem be reinforced against strains predominantly imposed by self-loading and wind gusts (Niklas, 1992; Spatz and Bruechert, 2000), and possible additional strains from things such as snow, lianas, and epiphytes. Unlike shoots, roots are often oriented horizontally and are held in the surrounding soil substrate, and this alters their mechanical environment and the stresses they experience. The material properties of wood can be characterized by stiffness (modulus of elasticity, MOE) and strength to resist breakage (modulus of rupture, MOR; Jacobsen *et al.*, 2005). Xylem strength and stiffness can vary greatly and changes in these traits are often associated with changes in xylem density (van Gelder *et al.*, 2006; Jacobsen *et al.*, 2007).

Tree xylem stores and releases water as a result of fluctuating water potentials, which most commonly occurs with diurnal transpiration. Water stored in the xylem can be released into the transpiration stream to help maintain safe transport conditions in angiosperms that are relatively sensitive to cavitation (Tyree and Ewers, 1991; Meinzer et al., 2008, 2009). The relationship between the loss of stored water and water potential of the xylem can be evaluated through moisture-release curves (Richards *et al.*, 2014; Jupa *et al.*, 2016) and by assessing such curves the amount of water released per unit water potential can be calculated to determine the hydraulic capacitance (Pratt and Jacobsen, 2017). Woody trees with higher capacitance typically have greater access to stored water (Richards *et al.*, 2014), whilst trees that are relatively more tolerant to dehydration are less dependent on capacitance (Scholz *et al.*, 2007; Meinzer *et al.*, 2009). Higher xylem water storage is associated with reductions in both biomechanical strength and xylem density within woody plants (Chapotin *et al.*, 2006; Pratt *et al.*, 2007).

The density of xylem (dry mass per volume) is a bulk tissue property that has been used to evaluate xylem function (e.g. Hacke *et al.*, 2001; Woodrum *et al.*, 2003; Jacobsen *et al.*, 2007; Utsumi *et al.*, 2010; Pratt and Jacobsen, 2017) in addition to many other aspects of tree function, such as growth rate (King *et al.*, 2005; van Gelder *et al.*, 2006) and pathogen resistance (Augspurger and Kelly, 1984; Alvarez-Clare and Kitajima, 2007). Xylem density is associated with xylem biomechanical strength (Panshin and de Zeeuw, 1980) and the ability to resist vessel implosion under negative hydraulic pressure (Hacke *et al.*, 2001; Jacobsen *et al.*, 2005). Lower xylem density potentially allows more water to be stored in the xylem tissue (Pratt and Jacobsen, 2017).

Most studies examining xylem functional trade-offs have used a comparative approach, with many different species being examined within a single study (reviewed by Pratt and Jacobsen, 2017 and Venturas *et al.*, 2017). A smaller number of studies have examined xylem functional trade-offs between different populations of a single species (e.g. Bouffier *et al.*, 2003; Barnard *et al.*, 2011; Medeiros and Pockman, 2014). These types of inter- and intraspecific studies have often examined the xylem of distal stems; however, xylem composition is not constant within trees (Domec and Gartner, 2001, 2002; Domec *et al.*, 2009; McCulloh *et al.*, 2014; Johnson *et al.*, 2016; Jacobsen *et al.*, 2018; Olson *et al.*, 2021), especially between roots and shoots (Alder *et al.*, 1996; Kavanagh *et al.*, 1999; Hacke *et al.*, 2000; McElrone *et al.*, 2004; Pratt *et al.*, 2007; Plavcová *et al.*, 2019). While these studies are ecologically informative, they are often difficult to interpret because of differences in tissue composition between species and because only partial information on whole-plant function is available due to limited sampling within each plant (most often only distal stems).

A complementary approach to understanding functional trade-offs within the xylem is to use within-plant (i.e. intra-organismal) differences to evaluate xylem functions and their relationships (Sperry and Saliendra, 1994; Domec and Gartner, 2001; Jacobsen *et al.*, 2018). Using such an approach controls for many of the differences in cell type and cellular arrangement that occur between species while still permitting xylem with a range of functional features to be compared. This sampling approach also provides information on functions from many locations within the whole plant. Given the large size of woody trees, the demands of long-distance transport, and the different mechanical environments of roots compared to self-supporting shoots, it is likely that xylem function varies greatly throughout the plant body; however, this has not been extensively examined and previous studies have typically compared only one position/sample size within roots and shoots (Pratt *et al.*, 2007; Jupa *et al.*, 2016; Plavcová *et al.*, 2019). Intra-organismal studies are valuable in describing the range of xylem functions that a plant is capable of producing, and this information in turn is useful in understanding the potential for selection to alter traits (Olson, 2012; Rosell *et al.*, 2012)

In the present study, we examined intra-organismal variability in the xylem traits of density, biomechanics, and water storage at different positions within the tree body of a model angiosperm species. We hypothesized that variability in xylem traits occurs within trees in response to the different biomechanical stresses on shoots and roots and the different water potential gradients that occur within plants from root to leaf. We predicted that there would be large differences in xylem functional traits between root and shoot samples (Pratt *et al.*, 2007; Domec *et al.*, 2009; Jupa *et al.*, 2016), because these organs experience vastly different environments; that xylem traits would differ within organs (e.g. within the shoot or within the root) depending upon organ diameter and/or position within the organ, because

the functional demands on distal positions, such as small twigs, may differ greatly from wide, older positions, such as the tree bole (Sarmiento *et al.*, 2011; McCulloh *et al.*, 2014; Johnson *et al.*, 2016); and that there would be functional trade-offs within the xylem, especially between biomechanical and water-storage functions (Niklas *et al.*, 2000; Chapotin *et al.*, 2006; van Gelder *et al.*, 2006).

## Material and methods

### *Plant material*

Xylem was sampled from the model tree species *Populus balsamifera* L. subp. *trichocarpa* (Torr. & A. Gray ex. Hook.; Salicaceae, black cottonwood; poplar) (Jansson and Douglas, 2007). All trees were grown on the campus of California State University, Bakersfield (CSUB) in the Environmental Studies Area (ESA) (see Jacobsen *et al.*, 2019 and Venturas *et al.*, 2019 for additional details). Six trees were sampled during summer 2016 (June–July), when they were 9 years old. Some additional tests and follow-up measurements were conducted during summer 2017 from trees within the same research plot. Trees were excavated by hand using mostly small trowels and soil knives, and with the assistance of many individuals working simultaneously. Trees did not have a taproot and we found no roots that extended more than 2 m depth into the soil, with most roots occurring within the upper 1 m of soil. The entire root zone was excavated, working from the tree base outward to root tips, so that the longest root could be identified for sample collection. There were usually several co-dominant roots of similar diameter and length

For each tree, xylem was sampled from along the tallest shoot and the longest root. The trees were relatively uniform in size, with a mean shoot height of 5.46±0.22 m (±SE) and a mean maximum root length of 6.45±0.35 m. The root–shoot junction was designated as the '0 m' position and xylem samples were collected beginning at 0.5 m below (–0.5 m for roots) and above (0.5 m for shoots) this point. Samples were then taken at 1-m intervals all the way up the main shoot and all the way down the longest root. We chose to sample at evenly spaced intervals so that it was representative of tissue distribution along the root-to-shoot axis. We were also particularly interested in the older proximal root and shoot samples because such locations have only rarely been studied, and hence we did not follow the apex-intensive sampling that has been used in some recent studies of vessel diameter (e.g. Soriano *et al.*, 2020). Roots were often longer than shoots, resulting in more sampled root positions than shoot positions based on our 1-m sampling scheme (total root samples=37, total stems=32). At each sample position, the organ diameter was measured and a 0.5-m length of intact xylem was excised, centered on the sampling point. The sampled segments were excised with a saw for large diameter samples and with shears for smaller diameter samples. Segments were immediately placed in large buckets, submerged in water, and transported back to the laboratory for additional processing (<2 h from excision).

Each sampled segment was divided into two equal 0.25-m proximal and distal sections, and these were further trimmed as described for the measurements below. The proximal sections were used for biomechanical and density measurements whilst the distal sections were used for measurements of capacitance. Similar to Domec and Gartner (2001), samples of shoots/roots from positions with large diameters (>1 cm) were split longitudinally and whittled into ~1-cm diameter cylinders of xylem. These were shaped out of the xylem closest to the bark to capture predominantly current-year growth. The vast majority of samples were whittled cylinders, with only some of the most distal samples being narrower than 1 cm. We did not find any differences between whittled and intact distal samples in our biomechanics measures (see Results). For the other, non-biomechanical traits, only current-year xylem was measured (with no bark or pith) regardless of the diameter of the sample position, and hence all these samples consisted of similar excised xylem segments regardless of position within the tree.

### *Biomechanics and xylem density*

Proximal xylem segments were trimmed to 0.20 m in length and ~1 cm in diameter and were loaded into a material properties tester (Instron Model 3342, Norwood, MA, USA), with parameters set for a 4-point bending test to produce a deformation response-to-load curve (Fig. 1). The modulus of rupture (MOR; strength to resist breakage) and the modulus of elasticity (MOE; stiffness) were then derived from the curves. These parameters were calculated with corrections for the area of tissue measured, so they represent the mechanical properties of the tissue. This differs from the mechanical properties of the intact shoot/root location, which will depend on both the properties of the tissue and the amount (diameter) of tissue present at a given location within the tree body. All calculations were performed according to Jacobsen *et al.* (2005).

Following the biomechanical tests, a 2-cm long section of undamaged tissue was excised from the end of each sample and used for determination of the xylem density. The xylem tissue was saturated using vacuum-infiltration for >12 h and the volume was calculated from the mass displacement of the sample when it was submerged in water of known temperature and density. The samples were then dried in an oven at 60 °C for ≥72 h and weighed to determine dry mass. The xylem density was calculated as the saturated volume divided by the dry mass.

### *Native water potentials in root and shoot xylem*

The range of xylem water potentials experienced within the trees between dawn and midday was measured during August–September 2016. Water potentials were measured at pre-dawn (05.30–06.30 h) and again at midday (12.00–13.00 h) on roots and shoots at 0.5, 2.5, and 4.5 m from the root–shoot junction. All samples for an individual tree were collected on the same day, but different trees were measured on different days because of the time required to excavate the root samples. In contrast to the protocol for our other xylem samples, which were collected following excavation of entire trees, the samples for water potential were

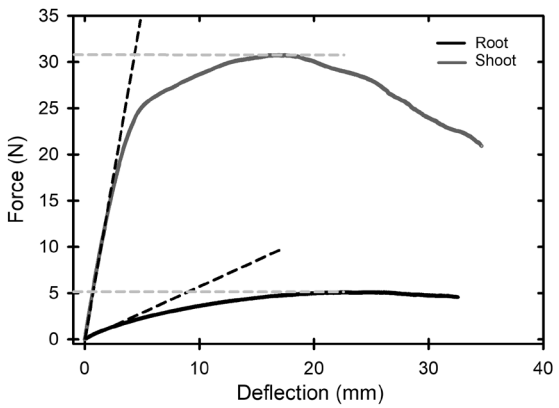


**Fig. 1.** Representative curves from four-point bending tests for roots (solid black line) and shoots (solid dark grey line) of 9-year-old trees. The modulus of elasticity (MOE, stiffness) is derived from the slope of the initial linear portion of the curve (dashed black line) and the modulus of rupture (MOR, strength to resist breakage) is derived from the maximum force (dashed grey line), both according to Jacobsen *et al.* (2005). The examples shown are from the same tree, both at 4.5 m away from the root–shoot junction.

not necessarily from the longest root. Instead, samples were taken from a single, dominant root that was excavated only up to 4.5 m from the root–shoot junction, leaving most of the soil undisturbed, including around the root tip. The distal shoot and root positions (i.e. 4.5 m from the junction) were relatively narrow in diameter and were sampled using shears. A smaller section of xylem was removed from these segments in the lab. The other, proximal positions were sampled using a 12-mm diameter increment borer to extract a piece of xylem tissue ~1 cm wide. The water potentials of the xylem samples were measured using a calibrated dew-point hygrometer (WP4C Water Potential Meter, Decagon Devices, Pullman WA, USA), and the ranges were used to inform our analyses of xylem capacitance as described below.

### *Water storage*

Xylem moisture-release curves (MRC) are time-consuming to generate and hence it was not possible to measure all of the samples that were harvested simultaneously from each excavated tree. Therefore, we confined our measurements to the root and shoot samples taken at 0.5, 2.5, and 4.5 m from the root–shoot junction. Xylem samples of the current-year growth were trimmed to 2 cm in length, separated from the bark, and, if required, split longitudinally for removal of the pith (final width ~0.5 cm; 6 replicate trees were measured at 6 sampling positions each for a total of 36 samples). The tissue samples were saturated overnight (>12 h) using vacuum-infiltration and then dried to remove free water by lightly dabbing with Kimwipes (Kimberly-Clark) before being weighed on analytical balance to obtain the saturated mass.

The MRCs were constructed by monitoring the water potential and mass of the samples as they dehydrated from saturation. The water potentials were measured using the WP4C dew-point hygrometer as described and tested by Baer (2018), and the samples were weighed before and after being inside the hygrometer chamber to determine a mean mass (Meinzer *et al.*, 2003). Measurements were taken repeatedly as the samples were allowed to slowly dehydrate on a benchtop until they reached water potentials lower than those observed in living *P. balsamifera* subsp. *trichocarpa* (with 10 to more than 20 measures taken to generage the curve for each individual sample). The samples were then oven-dried at 60 °C for ≥72 h to determine dry mass. We used the measurements of mass to calculate changes in both the relative water content (RWC) and the cumulative water loss (CWL), the latter being the amount of water lost per wood volume (Jupa *et al.*, 2016). RWC and CWL values were both used to construct two separate moisture-release curves for each xylem sample.

Different methods have been used to analyse MRCs (McCulloh *et al.*, 2014; Richards *et al.*, 2014; Jupa *et al.*, 2016; Meinzer *et al.*, 2003). In this study, the MRCs were partitioned into three phases according to the changes that were observed in the rate of water loss with decline in water potential (Fig. 2). The linear portion (Phase 2) of the curve generally occurred between -0.5 and -1.5 MPa, but this varied across samples. From within this initial water potential range, additional points were included or excluded within Phase 2, so that the analyzed linear portion of the cuve included the maximum number of points that simultaneously maximized the strength of the linear curve fit. We focused on the second phase of the curve because this was consistent with native water potential ranges experienced in the field by the trees that we sampled and it was the phase that showed a linear relationship between water potential and CWL (however, see Meinzer *et al.*, 2003). Capacitance (the amount of water released per unit water potential) was calculated from a fitted single major-axis regression of the linear phase of the curve generated for each of the two storage metrics of CWL ($C$) and RWC ($C_{RWC}$). The water potential at the Phase 2 to 3 transition ($P_{2-3}$) was considered the point at which xylem water storage was effectively depleted, where continued water loss would exponentially lower the water potential in the xylem. A fitted single major-axis regression of the data within Phase 3 was used to find the $y$-intercept that represented the total water-storage capacity of the xylem ($S$; Fig. 2). The functional amount of water storage ($S_f$) was defined as the difference in CWL values between the beginning and end of Phase 2.

### *Visual assessment of water storage using microCT*

Measuring xylem water storage typically involves the excision of samples; however, if intact vessel lumens are opened during sampling, as is likely in angiosperms, a portion of the water-storing component of the xylem may be altered compared to the undisturbed state. It has been demonstrated that vessels contribute to water storage discharge during pressure decline (Hölttä *et al.*, 2009; Pratt and Jacobsen, 2017), so opening vessels may affect xylem water storage properties. However, the WP4C instrument we used for MRC measurements has a larger sampling chamber than other common psychrometers, which allowed us to use much longer samples than most previous studies. *Populus balsamifera* subsp. *trichocarpa* has relatively short vessels, and hence this extra sample length is important for minimizing errors associated with vessels being cut open (Pratt and Jacobsen, 2017). Nevertheless, we also used high-resolution computed tomography (microCT) to observe stem xylem tissue in its intact state and combined this with water potential measurements to evaluate whether capacitance as measured on segments was representative of *in situ* functioning in intact xylem.

Large lateral branches of >1 m length were collected from trees growing adjacent to the ones used for the sampling described above (i.e. same age and cohort). Branches from $n$=5 replicate trees were collected at pre-dawn, double-bagged in large plastic bags, and brought back to the laboratory. For each branch, leaves from smaller lateral branches ($n$=4 per branch) were bagged within the larger plastic bags so that leaf and xylem water potential could equilibrate. These leaves were located >30 cm

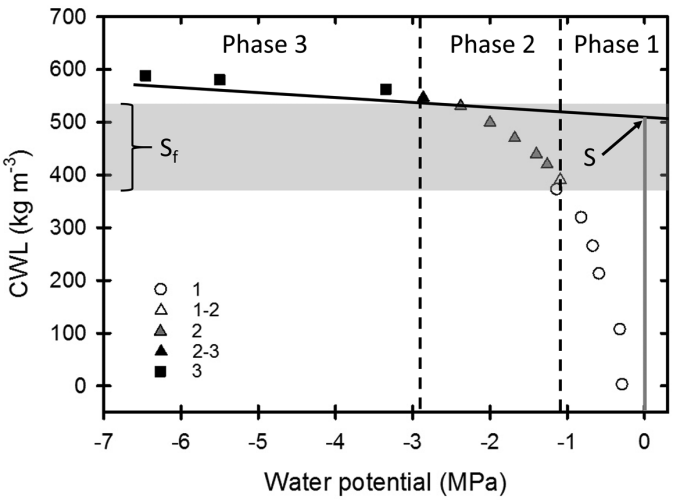


**Fig. 2.** Representative moisture release curve showing the relationship between cumulative water loss (CWL) and water potential inside of a xylem sample. The curve has three phases, which are separated by the dashed lines. Points that delineate phases represent phase transitions (1–2 and 2–3) and these were water potential values that were used within comparisons. The $y$-intercept of the Phase-3 slope was used to determine the total water storage capacity of the xylem, $S$. The functional amount of water storage ($S_f$) was determined as the cumulative water loss of Phase 2 (grey shading bound by the Phase 1-2 and 2-3 triangular points), and this was considered to be an important trait because this corresponded to the range of water potentials that trees experienced in the field. The data in this curve are from a root xylem sample located 0.5 m from the root–shoot junction.

away from the region to be scanned. After 4 h of equilibrating, branch xylem water potential was estimated by measuring the equilibrated leaf water potential using a pressure chamber (Model 2000, PMS Instrument Company, Albany, OR, USA). The native water potentials of the scanned samples ranged from –0.6 to –1.4 MPa and were consistent with the range of native water potentials measured in field-grown trees.

After the estimation of the branch water potential, we selected a straight, distal stem of ~25-40 cm in length and cut it from the branch, leaving its apical end intact. The total length of these samples was limited by the chamber size of the microCT, which could accommodate stems only up to 50 cm. The length of our samples was greatly in excess of the mean length of xylem vessels in the trees from our study plot, which has previously been reported as 1.8 cm (Jacobsen *et al.*, 2019). The cut end of each stem was sealed with plastic wrap and the sample was scanned for 15–20 min at ~15–20 cm from the cut end in a region of the stem that was ~6–10 mm diameter using a microCT scanner (Skyscan 2211, Bruker Corporation, Kontich, Belgium).

The scanned portion of the stem was then excised for further analyses. A 2-cm section was used to cut thin hand-sections for light microscopy. The remainder of this section (i.e. most of it) was dried at room temperature for >5 d and re-scanned to evaluate the changes in the cell wall components. A separate 3-cm section, sampled adjacent to the 2-cm one, was excised and used to create a MRC as described above.

The paired scans of fresh and dried stems were analysed using microCT analysis software (CTAn v.1.13, Bruker Corporation, Kontich, Belgium). From each scanned volume, a single digital transverse section was selected from the center of the scanned region for image analysis. The sections were binarized to delineate air (black in images) from solids and liquids (grey in images) as detected by their X-ray absorption. Sections were compared to light micrographs to ensure that thresholding and binarization of images were consistent with the structure of the xylem matrix. The microCT images were used to calculate the native fraction of water volume in the fresh samples, assuming all the vessel and fiber lumen volume within the stem could potentially store water. From the dried xylem sample and the native xylem sample the percentage of native wall area in the sample was estimated. The proportion of cell wall within native samples was calculated using the percentage of dry wall within the dried xylem sections relative to the total xylem area. We applied this value from dried samples, which had high contrast between air-filled lumens compared to cell walls within scans, to calculate the area that corresponded to the same percentage of total sample size within native samples. The cell wall area corresponded to area that could not release stored water, and the remaining xylem area was calculated to represent the space within the native sample that could potentially store water. For each native sample, the proportion of X-ray absorbing area (cell wall and water) was measured and the cell wall area subtracted out using the calculation described above. This allowed us to estimate the native water fraction within the lumens of cells within samples. The relative water content (RWC) from microCT images was calculated using the native water fraction divided by the area within the xylem that could potentially store water (i.e. the non-cell-wall component).

RWC from microCT analyses were compared to MRC from their paired xylem segments. A paired *t*-test was used to compare RWC calculated from the MRC and microCT at the native water potential of the scanned branch.

### Statistical analyses

Differences between the xylem functioning of roots and shoots were examined using Minitab (v.17). Relationships between xylem traits were examined across and within these organs using Pearson correlation coefficients. A two-way mixed model ANOVA was used to determine whether organ influenced xylem biomechanics (MOR, MOE), density, and water-storage properties ($P_{2-3}$, $C$, $C_{RWC}$, $S$, $S_f$). Organ, tree, and tree × organ interaction were included in the model.

We analysed the data in several different ways to examine changes in traits along the root–shoot axis. First, we looked at patterns based on the sample positions in relation to the root–shoot junction. Second, we used the total shoot and root lengths from each tree to examine traits relative to their positions from the root and shoot apices (Olson *et al.*, 2020). For this analysis, the sample distance from the root–shoot junction (R–S) was divided by the total length of the organ to determine its relative position. This parameter was termed the organ length fraction (OLF) position, and OLF values ranged from –1 at the root tip to +1 at the shoot tip. Third, we also analysed data relative to the organ diameter at each sampled position, as in Jacobsen *et al.* (2018). This analysis was very similar to that for OLF because the organs tapered along their length (Supplementary Fig. S1). A full factorial ANCOVA model was used to determine whether the xylem traits correlated with OLF and organ diameter across all samples and within the individual organs, with tree as a random factor and organ as a fixed factor. The model was performed with four interaction terms: tree × organ, covariant × tree, covariant × organ, and covariant × tree × organ. Parametric assumptions were assessed for each group of the model.

## Results

### Biomechanics and xylem density

The biomechanical traits of the xylem greatly differed between the roots and shoots (Fig. 1, Tables 1, 2). Stem xylem was significantly stiffer (~63%) and stronger (~60%) than root xylem. For roots, both stiffness (MOE) and strength to resist breakage (MOR) increased as organ diameter increased, whereas shoots showed the opposite pattern with strength and stiffness increasing as organ diameter decreased (Fig. 3D, F, Table 3,). This resulted in increases in xylem strength and stiffness along a continuum from the root tip to shoot tip (Fig. 3C, E). Shoots displayed a noticeable decline in strength in more narrow and distal positions, past 0.75 OLF (Fig.

**Table 1.** Biomechanical and water storage traits of root and shoot xylem

| Organ | MOE (N mm$^{-2}$) | MOR (N mm$^{-2}$) | Xylem density(kg m$^{-3}$) | $P_{1-2}$(MPa) | $P_{2-3}$(MPa) | C(kg m$^{-3}$ MPa$^{-1}$) | $C_{RWC}$(RWC MPa$^{-1}$) | S(kg m$^{-3}$) | $S_f$(kg m$^{-3}$) |
|---|---|---|---|---|---|---|---|---|---|
| Shoot | 3928±248 | 90.5±4.2 | 430.9±6.6 | –0.65±0.05 | –1.59±0.11 | 132.8±10.8 | 0.20±0.011 | 389.7±13.4 | 114.4±10.3 |
| Root | 1440±154 | 36.0±3.0 | 262.3±5.1 | –0.64±0.05 | –1.49±0.03 | 149.7±11.5 | 0.22±0.02 | 501.8±16.0 | 120.7±11.8 |

Biomechanical traits (see Fig. 1): MOE, modulus of elasticity; MOR, modulus of rupture. Water-storage traits (see Fig. 2): $P_{1-2}$, water potential at the start of Phase 1; $P_{2-3}$, water potential at effective storage depletion; $C$, capacitance in relation to cumulative water loss; $C_{RWC}$, capacitance in relation to relative water content; $S$, water storage at effective storage depletion; $S_f$, functional amount of water storage. Data are means (±SE) of $n$=37 for roots and $n$=32 for shoots.

**Table 2.** Two-way ANOVA of xylem biomechanical traits compared between root and shoots, and between trees

| | | MOE | | MOR | | Xylem density | |
|---|---|---|---|---|---|---|---|
| **Factor** | **d.f.** | ***F*** | ***P*** | ***F*** | ***P*** | ***F*** | ***P*** |
| Organ (root, shoot) | 1,57 | 121.42 | **<0.001** | 950.03 | **<0.001** | 239.23 | **<0.001** |
| Tree | 5,57 | 1.52 | 0.329 | 5.62 | **0.041** | 1.15 | 0.440 |
| Organ × Tree | 5,57 | 0.58 | 0.716 | 0.10 | 0.991 | 1.97 | 0.097 |

MOE, modulus of elasticity; MOR, modulus of rupture (see Fig. 1). d.f., degrees of freedom. Significant effects ($P<0.05$) are highlighted in bold.

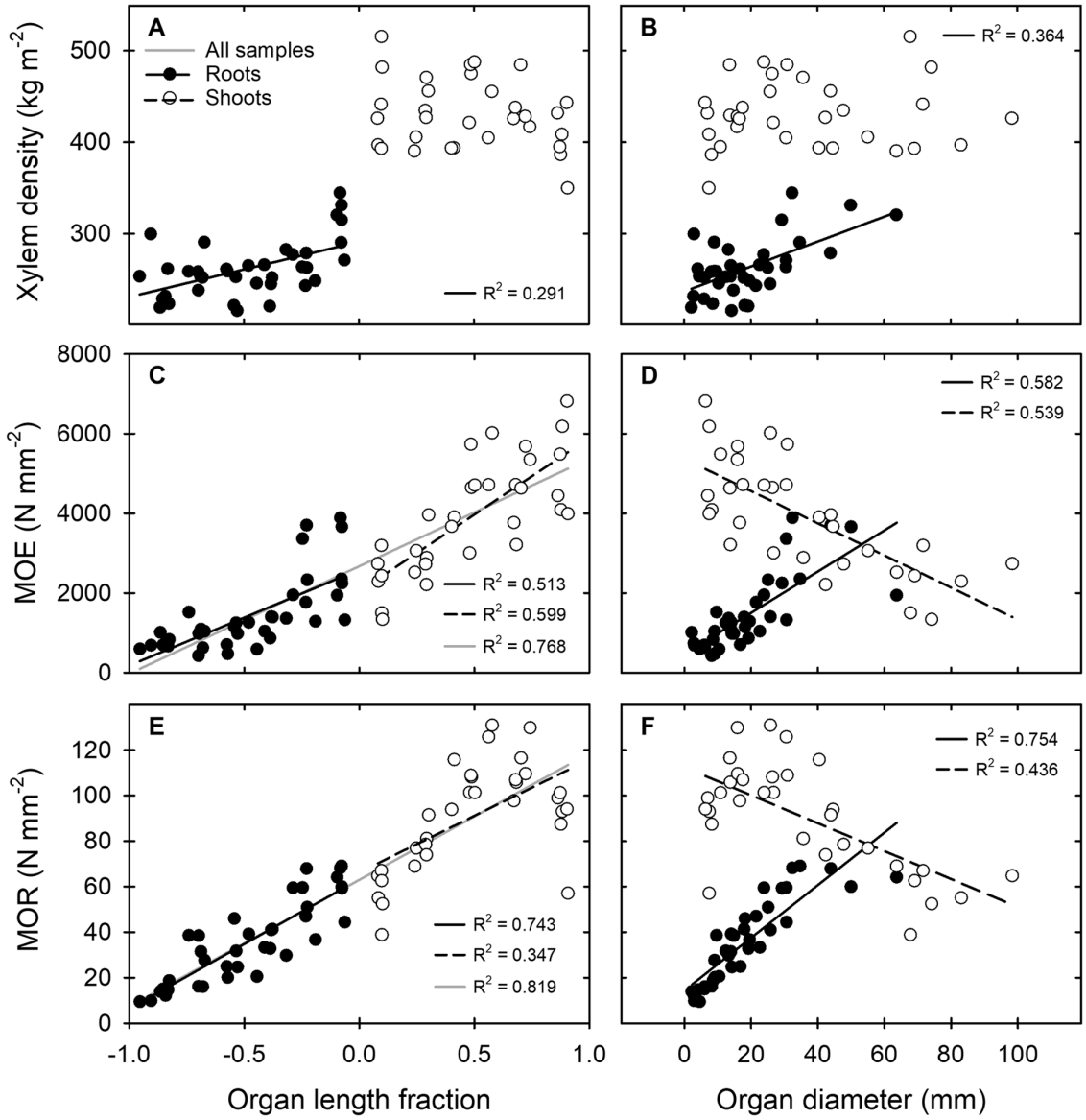


**Fig. 3.** Variations in xylem density, stiffness, and strength in roots and shoots of 9-year-old trees in relation to distance from the root–shoot junction (A, C, E) and organ diameter (B, D, F). Stiffness is shown as the modulus of elasticity (MOE), and strength to resist breakage is shown as the modulus of rupture (MOR). The organ length fraction was calculated as the distance of the sample from the root–shoot junction divided by the total length of the organ (root or shoot), where –1 represents the root apex and 1 represents the shoot apex. Lines are shown only for significant linear relationships and $R^2$-values are shown for significant correlations.

3E). Whilst whittled samples were used for most positions, some of the more distal ones were measured as intact roots and stems because of their small diameters. At the positions where we used a mixture of both whittled and intact samples (root –4.5 m, shoot 4.5 m) we found no significant differences between them in either MOE or MOR ($P>0.05$).

**Table 3.** Full factorial ANCOVA models for variation in root and shoot xylem biomechanical traits with organ diameter and distance from the root–shoot junction (organ length fraction)

| | | MOE | | MOR | | Xylem density | |
|---|---|---|---|---|---|---|---|
| **Covariant and factors** | **d.f.** | ***F*** | ***P*** | ***F*** | ***P*** | ***F*** | ***P*** |
| Covariant: Diameter | | | | | | | |
| Diameter | 1,45 | 31.49 | **>0.001** | 53.26 | **>0.001** | 14.68 | **>0.001** |
| Diameter × Tree | 5,45 | **2.77** | **0.029** | 2.08 | 0.085 | 0.50 | 0.772 |
| Tree | 5,45 | 0.94 | 0.525 | 0.63 | 0.687 | 1.46 | 0.345 |
| Diameter × Organ | 1,45 | 124.85 | **>0.001** | 122.74 | **>0.001** | 5.39 | **0.025** |
| Diameter × Tree × Organ | 5,45 | 4.77 | **0.001** | 3.49 | **0.009** | 0.74 | 0.600 |
| Organ | 1,45 | 166.43 | **>0.001** | 231.35 | **>0.001** | 223.38 | **>0.001** |
| Tree × Organ | 5,45 | 2.03 | 0.093 | 1.25 | 0.301 | 1.10 | 0.373 |
| Covariant: Organ length fraction (OLF) | | | | | | | |
| OLF | 1,45 | 105.71 | **>0.001** | 106.58 | **>0.001** | 1.99 | 0.165 |
| OLF × Tree | 5,45 | 1.50 | 0.208 | 0.37 | 0.863 | 2.31 | 0.059 |
| OLF × Organ | 1,45 | 4.74 | **0.035** | 24.77 | **>0.001** | 18.82 | **>0.001** |
| OLF × Tree x Organ | 5,45 | 1.91 | 0.112 | 0.36 | 0.871 | 0.81 | 0.549 |
| Organ | 1,45 | 2.24 | 0.194 | 6.56 | 0.050 | 35.00 | **0.002** |
| Tree × Organ | 5,45 | 1.40 | 0.244 | 0.26 | 0.932 | 4.21 | **0.003** |

MOE, modulus of elasticity; MOR, modulus of rupture (see Fig. 1). d.f., degrees of freedom. The organ length fraction was calculated as the distance of the sample from the root–shoot junction divided by the total length of the organ (root or shoot). Significant effects ($P$<0.05) are highlighted in bold.

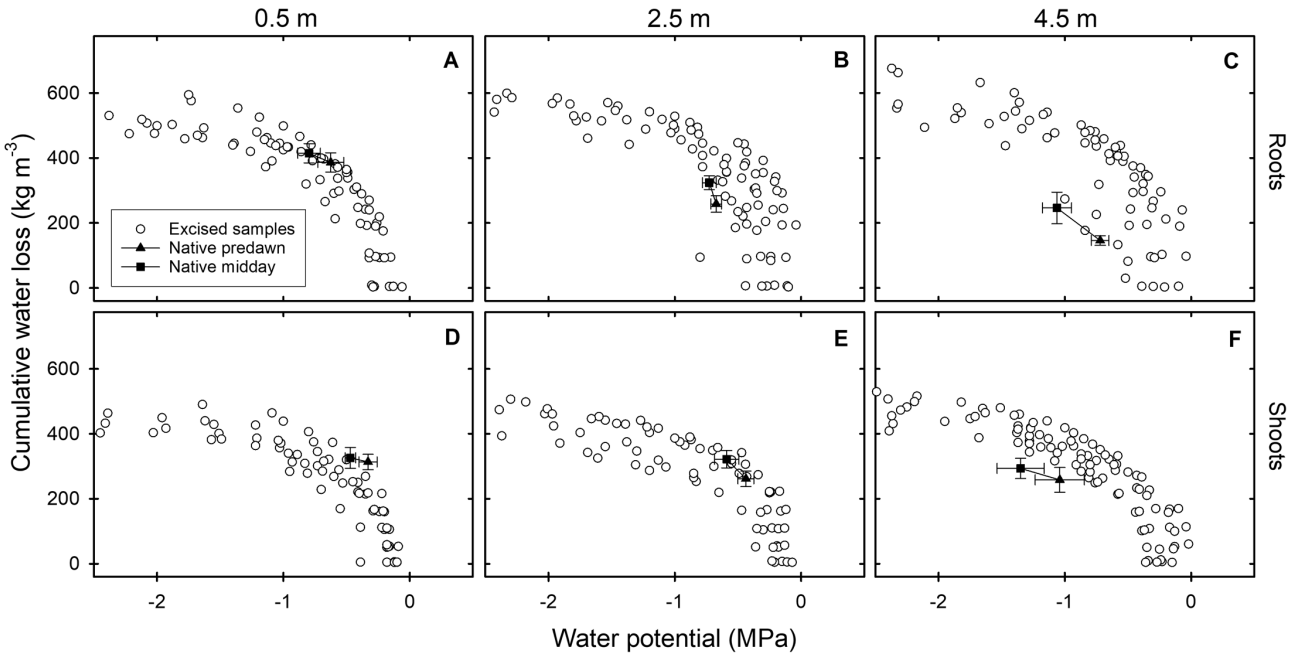


**Fig. 4.** Moisture-release curves for xylem in the roots and shoots of 9-year-old trees. The curves show relationship between cumulative water loss and water potential for (A–C) root and (D–F) shoot samples located at different distances from the root–shoot junction. The open symbols indicate excised xylem samples measured in the laboratory and the closed symbols indicate *in situ* measurements taken at pre-dawn and midday in the field ('native'). Open symbols are individual data-points and closed symbols are means (±SE) of $n$=6 replicates.

Roots had ~40% lower xylem density than shoots (Tables 1, 2), and the density increased as root diameter increased (Fig. 3B). In contrast to strength and stiffness, xylem density did not display a continuous increase along the main root–shoot (Fig. 3A). Instead, there was an abrupt transition between considerably different values for the roots and shoots.

### *Water storage*

Moisture-release curves were used to evaluate the loss of water from the xylem with declining water potential (Fig. 4; curves for individual trees are given in Supplementary Fig. S2). Native water potentials measured in trees in the field were within the

**Table 4.** Two-way ANOVA of xylem water-storage traits compared between root and shoots, and between trees

| | | $P_{2-3}$ | | $C$ | | $C_{RWC}$ | | $S$ | | $Sf$ | |
|---|---|---|---|---|---|---|---|---|---|---|---|
| **Factor** | **d.f.** | ***F*** | ***P*** | ***F*** | ***P*** | ***F*** | ***P*** | ***F*** | ***P*** | ***F*** | ***P*** |
| Organ (root, shoot) | 1,24 | 0.24 | 0.647 | 1.68 | 0.252 | 0.80 | 0.411 | 19.14 | **0.007** | 0.14 | 0.726 |
| Tree | 5,24 | 7.28 | **0.024** | 0.78 | 0.604 | 1.28 | 0.397 | 0.52 | 0.753 | 0.92 | 0.535 |
| Organ × Tree | 5,24 | 0.16 | 0.975 | 1.40 | 0.260 | 0.93 | 0.480 | 1.60 | 0.198 | 1.24 | 0.322 |

$P_{2-3}$, water potential at effective storage depletion (see Fig. 2); $C$, capacitance in relation to cumulative water loss; $C_{RWC}$, capacitance in relation to relative water content; $S$, water storage at effective storage depletion; $S_f$, functional amount of water storage. d.f., degrees of freedom. Significant effects ($P$<0.05) are highlighted in bold.

**Table 5.** Full factorial ANCOVA models for variation in root and shoot xylem water-storage traits with organ diameter and distance from the root–shoot junction (organ length fraction)

| | | $P_{2-3}$ | | $C$ | | $C_{RWC}$ | | $S$ | | $Sf$ | |
|---|---|---|---|---|---|---|---|---|---|---|---|
| **Covariant and factors** | **d.f.** | ***F*** | ***P*** | ***F*** | ***P*** | ***F*** | ***P*** | ***F*** | ***P*** | ***F*** | ***P*** |
| Covariant: Diameter | | | | | | | | | | | |
| Diameter | 1,12 | 0.91 | 0.360 | 2.08 | 0.175 | 2.57 | 0.135 | 0.55 | 0.474 | 1.25 | 0.286 |
| Diameter × Tree | 5,12 | 4.30 | **0.018** | 1.61 | 0.230 | 8.53 | **0.001** | 1.37 | 0.303 | 0.52 | 0.758 |
| Tree | 5,12 | 0.83 | 0.580 | 0.37 | 0.852 | 0.71 | 0.642 | 0.67 | 0.662 | 0.55 | 0.738 |
| Diameter × Organ | 1,12 | 0.60 | 0.453 | 0.01 | 0.935 | 0.10 | 0.757 | 1.30 | 0.276 | 0.37 | 0.552 |
| Diameter × Tree × Organ | 5,12 | 5.20 | **0.009** | 3.16 | **0.048** | 12.73 | **>0.001** | 1.68 | 0.215 | 0.51 | 0.766 |
| Organ | 1,12 | 0.02 | 0.895 | <0.01 | 0.967 | 0.06 | 0.818 | 8.27 | **0.033** | 1.09 | 0.336 |
| Tree × Organ | 5,12 | 3.46 | **0.036** | 2.96 | 0.057 | 10.92 | **>0.001** | 2.01 | 0.149 | 0.49 | 0.780 |
| Covariant: Organ length fraction (OLF) | | | | | | | | | | | |
| OLF | 1,12 | <0.01 | 0.993 | 0.33 | 0.578 | 0.40 | 0.540 | 0.98 | 0.341 | 0.51 | 0.491 |
| OLF × Tree | 5,12 | 5.56 | **0.007** | 4.78 | **0.012** | 7.96 | **0.002** | 1.26 | 0.341 | 1.35 | 0.309 |
| Tree | 5,12 | 0.92 | 0.534 | 0.26 | 0.917 | 0.35 | 0.860 | 0.47 | 0.788 | 0.55 | 0.735 |
| OLF × Organ | 1,12 | 0.35 | 0.567 | 9.27 | **0.010** | 5.18 | **0.042** | 0.57 | 0.464 | 2.10 | 0.173 |
| OLF × Tree × Organ | 5,12 | 4.38 | **0.017** | 1.36 | 0.304 | 3.64 | 0.031 | 0.99 | 0.463 | 0.83 | 0.553 |
| Organ | 1,12 | 0.03 | 0.874 | 0.82 | 0.408 | 0.44 | 0.538 | 5.04 | 0.075 | 0.06 | 0.819 |
| Tree × Organ | 5,12 | 3.71 | **0.029** | 4.19 | **0.020** | 5.62 | **0.007** | 1.05 | 0.434 | 2.05 | 0.142 |

$P_{2-3}$, water potential at effective storage depletion (see Fig. 2); $C$, capacitance in relation to cumulative water loss; $C_{RWC}$, capacitance in relation to relative water content; $S$, water storage at effective storage depletion; $S_f$, functional amount of water storage. d.f., degrees of freedom. The organ length fraction was calculated as the distance of the sample from the root–shoot junction divided by the total length of the organ (root or shoot). Significant effects ($P$<0.05) are highlighted in bold.

range of values of Phase 2 within the MRCs (see Fig. 2), which provided further justification for our focus on this phase.

Roots and shoots differed in water storage capacity ($S$) but not in the other traits related to water storage (Table 4). The root xylem had significantly higher $S$ than that of the shoots (~25% more, equivalent to 100 kg $m^{-3}$; Tables 4, 5, Supplementary Fig. S3G, H). Roots had higher, less negative, water potentials associated with the upper and lower boundaries of Phase 2 that were used to calculate CWL, but the absolute ranges were similar (Supplementary Fig. S2) and thus the values for functional amount of water storage ($S_f$) were similar (Supplementary Fig. S3I, J, Tables 4, 5). Capacitance was not different between roots and shoots, either when expressed as CWL ($C$) or RWC ($C_{RWC}$) (Tables 4, 5, Supplementary Fig. S3C–F). The water potential at the point of exponential pressure loss ($P_{2-3}$) was also not different between the organs (Tables 4, 5, Supplementary Fig. S3A, B). Thus, the rate of water released per unit drop in pressure in Phase 2 of the MRC did not differ between roots and shoots, but the total amount of water released was higher in roots.

### *Xylem capacitance and visual analysis from microCT*

At native water potential, the RWC of large branches calculated from microCT analysis did not differ from that of trimmed xylem segments calculated from MRCs (Fig. 5; $t$=–0.72, $P$=0.512). One sample did show some divergence (bottom row in Fig. 5) and this differed from the others in being a very young apical stem segment. The microCT scans showed that there was a relatively large amount of gas within the xylem samples, even at relatively high water potentials ranging from –0.6 MPa to –1.4 MPa (Fig. 5).

Combining microCT images and light micrographs of the same sections allowed for the identification of vessels,

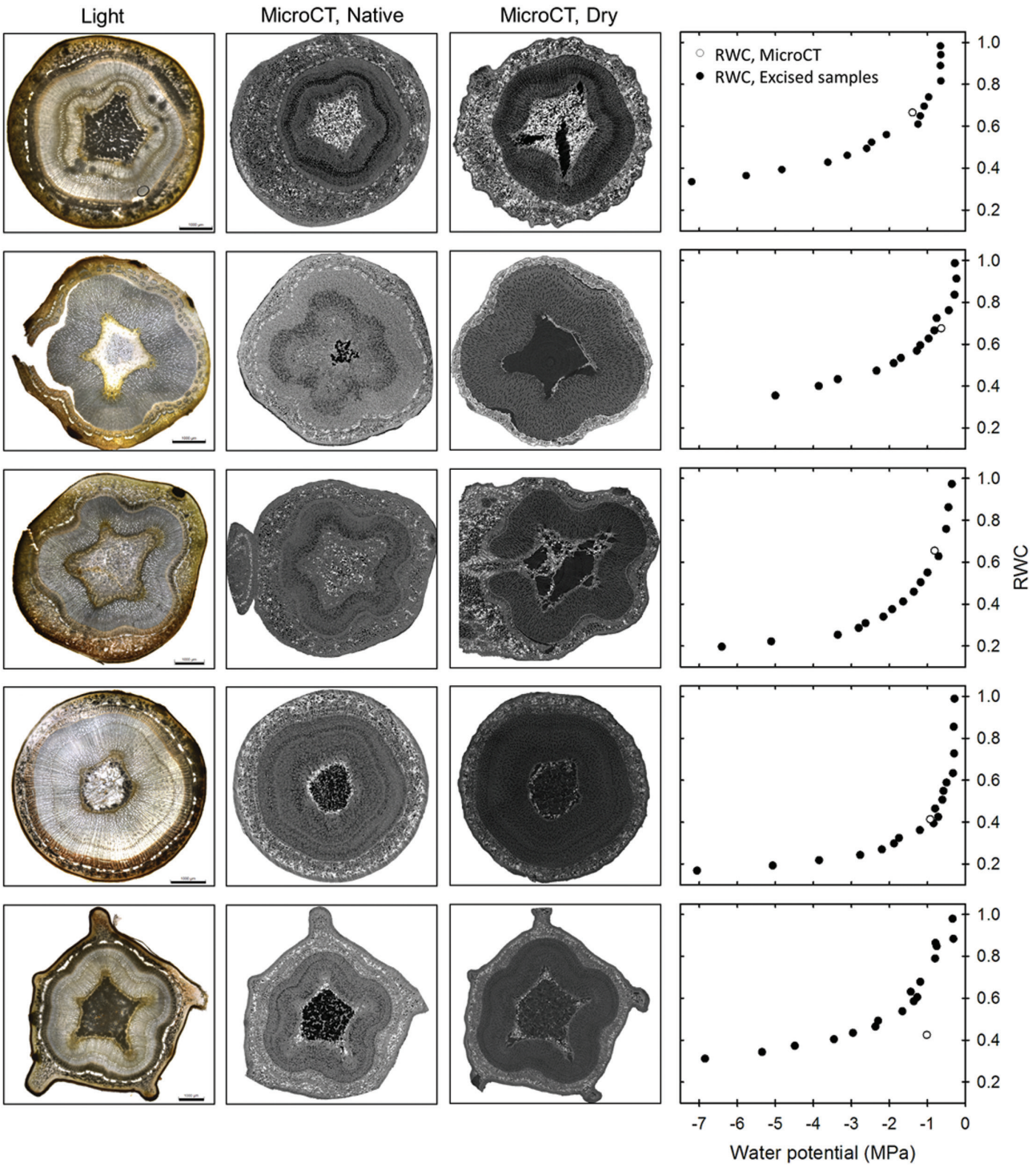


**Fig. 5.** Comparison of xylem moisture-release curves from excised tissues with native, intact samples imaged using high-resolution computed tomography (microCT) from the same stems of 9-year-old trees. The micrographs show transverse stem sections using light microscopy, and microCT scans from native, intact stems and from bench-dried stem segments ('dry'). Scale bars are 1 mm. The native and dry microCT scans were used to calculate the percentage of potential water-filled xylem space occupied in the fresh samples (open circles in the curves) compared to values of relative water content (RWC) determined from excised xylem samples (closed symbols).

fibers, and parenchyma rays (Fig. 5), especially when images were examined at high magnification. At the range of native water potentials of our samples, many fibers and vessels contained gas, indicating that released storage water was probably derived from both of these cellular components.

**Table 6.** Pearson correlations between xylem traits within the whole plant, and within roots and shoots only

| Group and trait | MOR | | MOE | | Density | | $P_{2-3}$ | | $C$ | | $C_{RWC}$ | | $S$ | |
|---|---|---|---|---|---|---|---|---|---|---|---|---|---|---|
| | $R^2$ | $P$ | $R^2$ | $P$ | $R^2$ | $P$ | $R^2$ | $P$ | $R^2$ | $P$ | $R^2$ | $P$ | $R^2$ | $P$ |
| **Root and shoot** | | | | | | | | | | | | | | |
| MOE | 0.930 | **<0.001** | | | | | | | | | | | | |
| Density | 0.811 | **<0.001** | 0.755 | **<0.001** | | | | | | | | | | |
| $P_{2-3}$ | –0.050 | 0.772 | –0.148 | 0.390 | –0.215 | 0.208 | | | | | | | | |
| $C$ | –0.225 | 0.186 | –0.184 | 0.282 | –0.320 | 0.057 | 0.566 | **<0.001** | | | | | | |
| $C_{RWC}$ | –0.101 | 0.558 | –0.082 | 0.635 | –0.166 | 0.333 | –0.646 | **<0.001** | | | | | | |
| $S$ | –0.636 | **<0.001** | –0.565 | **<0.001** | –0.703 | **<0.001** | 0.163 | 0.343 | 0.228 | 0.180 | 0.027 | 0.874 | | |
| $S_f$ | –0.101 | 0.557 | –0.004 | 0.981 | –0.098 | 0.572 | 0.486 | 0.003 | 0.275 | 0.104 | 0.141 | 0.412 | 0.324 | 0.054 |
| **Root only** | | | | | | | | | | | | | | |
| MOE | 0.914 | **<0.001** | | | | | | | | | | | | |
| Density | 0.563 | **<0.**001 | 0.624 | **<0.001** | | | | | | | | | | |
| $P_{2-3}$ | –0.081 | 0.750 | –0.265 | 0.288 | –0.084 | 0.739 | | | | | | | | |
| $C$ | –0.403 | 0.097 | –0.321 | 0.195 | –0.113 | 0.656 | 0.638 | **0.004** | | | | | | |
| $C_{RWC}$ | –0.183 | 0.468 | –0.164 | 0.516 | 0.043 | 0.865 | –0.733 | **0.001** | | | | | | |
| $S$ | –0.254 | 0.309 | –0.278 | 0.264 | –0.141 | 0.578 | 0.358 | 0.145 | –0.033 | 0.896 | –0.223 | 0.374 | | |
| $S_f$ | –0.388 | 0.112 | –0.106 | 0.676 | –0.156 | 0.537 | 0.635 | 0.005 | 0.029 | 0.910 | –0.158 | 0.531 | 0.496 | 0.049 |
| **Shoot only** | | | | | | | | | | | | | | |
| MOE | 0.758 | **<0.001** | | | | | | | | | | | | |
| Density | 0.048 | 0.795 | –0.015 | 0.934 | | | | | | | | | | |
| $P_{2-3}$ | 0.014 | 0.955 | –0.129 | 0.610 | –0.552 | **0.017** | | | | | | | | |
| $C$ | 0.235 | 0.349 | 0.220 | 0.379 | –0.409 | 0.092 | 0.438 | 0.069 | | | | | | |
| $C_{RWC}$ | 0.212 | 0.398 | 0.205 | 0.415 | –0.265 | 0.289 | –0.401 | 0.099 | | | | | | |
| $S$ | –0.296 | 0.233 | –0.136 | 0.590 | –0.449 | 0.061 | 0.017 | 0.947 | 0.281 | 0.258 | 0.130 | 0.608 | | |
| $S_f$ | 0.161 | 0.523 | 0.180 | 0.474 | –0.011 | 0.964 | 0.200 | 0.426 | 0.640 | **0.004** | 0.646 | **0.004** | 0.252 | 0.312 |

Biomechanical traits (see Fig. 1): MOR, modulus of rupture; MOE, modulus of elasticity. Water-storage traits (see Fig. 2): $P_{2-3}$, water potential at effective storage depletion; $C$, capacitance in relation to cumulative water loss; $C_{RWC}$, capacitance in relation to relative water content; $S$, water storage at effective storage depletion; $S_f$, functional amount of water storage. Significant effects ($P$<0.05) are highlighted in bold.

### *Trait correlations*

Both positive and negative correlations were observed between traits (Table 6), suggesting the presence of trade-offs. The biomechanical traits were strongly correlated with each other, both within and across the xylem of the roots and shoots (Fig. 6). Relationships between biomechanical traits and water storage parameters were mixed (Supplementary Fig. S4). Water storage capacity declined across roots and shoots as xylem density, MOR, and MOE increased, indicating a functional trade-off relationship between structural and storage traits. Neither of the capacitance traits $C$ and $C_{RWC}$ were correlated with tissue biomechanics or xylem density (Table 6).

Traits associated with water storage properties were generally correlated with each another, as were traits associated with capacitance, but these relationships varied slightly depending on organ type (Table 6, Supplementary Fig. S4). In the roots, greater functional water storage ($S_f$) was associated with more total xylem water storage ($S$) (Supplementary Fig. S4X) and reduced water potential at storage depletion ($P_{2-3}$) (Supplementary Fig. S4U). In shoots, increased $S_f$ was associated with more water released per unit pressure drop, with respect to both $C$ and $C_{RWC}$ (Supplementary Fig. S4V, W). Within roots and across both organs, lower $C$ and $C_{RWC}$ correlated with lower water potentials reached at water-storage depletion (Supplementary Fig. S4G, K). Water potentials were also lower at storage depletion as xylem density increased in the shoots (Supplementary Fig. S4C).

## Discussion

### *Xylem functioning differs in roots compared to shoots*

Xylem functional traits were found to vary within the plant body, with large differences between the roots and shoots. Shoot xylem had significantly higher density, strength to resist breakage (modulus of rupture, MOR), and stiffness (modulus of elasticity, MOE) than did root xylem, consistent with the different environments of these organs. The main shoot axis must continuously support its own weight and that of lateral branches against gravity and sporadically from wind. Roots also endure stresses transmitted down from the shoot, but the surrounding soil helps stabilize them against deflection. Pratt *et al.* (2007) observed that shallow shrub roots of Rhamnaceae do not differ in strength or stiffness compared to the shoots, but the far larger roots and shoots of *P. balsamifera* subsp. *trichocarpa* trees encounter greater mechanical stress and this might drive the need for biomechanical specialization of the xylem between the two organs.

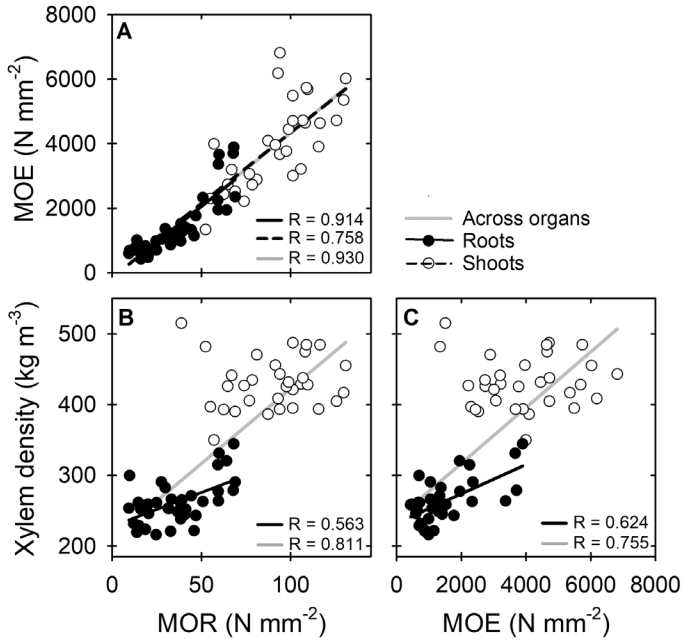


**Fig. 6.** Relationships between xylem density, stiffness, and strength in roots and shoots of 9-year-old trees. Relationships between (A) stiffness, shown as the modulus of elasticity (MOE), and strength to resist breakage, shown as the modulus of rupture (MOR), (B) xylem density and MOR, and (C) xylem density and MOE. Each data-point represents a single sample from a single position along the root–shoot axis within a tree. Lines are shown only for significant correlations and *R*-values are shown for significant correlations.

We found that roots had a higher water-storage capacity than the shoots, and storage capacity was correlated with xylem density across both roots and shoots. Lower xylem density would allow for more available space for water within the tissue (Pratt and Black, 2006). Roots are also closer to water stored externally in the surrounding soil, and so recharging their internal hydraulic supply would be less delayed compared to shoots. With more access to water stores than shoots, roots can probably support higher hydraulic conductivity (Kavanagh *et al.*, 1999) that is buffered from negative water potentials by water storage in the xylem tissue and the soil substrate (Meinzer *et al.*, 2009). The relatively limited overlap in the traits between roots and shoots that we found suggests different roles within the plant for these organs, and the influence of root traits on whole-plant functioning merits additional study (Sperry *et al.*, 1998; Domec *et al.*, 2006; Pratt *et al.*, 2010), especially for older roots that are rarely studied and are structurally different from younger, distal roots.

### *Xylem biomechanical traits vary along the root-to-shoot axis*

Within both roots and shoots, biomechanical traits varied along the main plant axis, with pronounced differences between proximal and distal samples within each. Xylem strength and stiffness both increased linearly across the organs from root tip to shoot tip (Fig. 3C, E). This contrasts with the log-linear pattern of increase in xylem vessel diameter that has been described for many species (Olson *et al.*, 2020; Soriano *et al.*, 2020). This suggests that some xylem structural and functional traits might be changing independently and that biomechanical changes are not directly linked to vessel structural changes within the shoot, although both change along the plant body axis.

In contrast to the biomechanical traits, xylem density did not change linearly and was relatively stable within the organs, but showed a large shift between the root and shoot tissues at their junction (Fig. 3A). The xylem in wider, older roots close to the root-to-shoot junction was particularly strong and stiff for their density. This region of roots in *Populus* trees has been described as the root plate (Stokes and Mattheck, 1996) and it probably functions to anchor the shoot, resist tension and compression of roots caused by wind stresses (Coutts, 1986), and prevent the tree from being uprooted.

In the shoots, xylem strength and stiffness increased as diameter declined toward the tree apex (Fig. 3D, F), and this pattern has also been observed in shoots of *Pseudotsuga menziesii* (Domec and Gartner, 2002). Improved strength and stiffness in smaller shoots may help protect them from mechanical damage caused by the more extreme conditions encountered at the margins of the tree crown (Butler *et al.*, 2012). Assuming constant tissue properties, the mechanical integrity of the shoot declines exponentially as the overall diameter decreases (Niklas, 1992); hence, increasing tissue-level MOE and MOR in narrow shoots might compensate for this effect.

### *Capacitance*

Under decreasing pressure, stored water is drawn first from locations of least resistance in the xylem matrix. Water release has been postulated to begin in the open spaces in the xylem matrix (Tyree and Yang, 1990; Tyree and Zimmerman, 2002; Borchert and Pockman, 2005; Ziemińska *et al.*, 2020). This concept has been supported in angiosperm trees, where greater fractions of vessels and fibers and larger lumen diameters of these cell types are correlated with higher capacitance, *C* (Jupa *et al.*, 2016). Our microCT scans showed that both fibers and vessels contained gas in intact branches (Fig. 5), indicating that released storage water was probably derived from both of these cellular components (Hölttä *et al.*, 2009), similar to what has previously been found during dehydration of the xylem in *Castanea dentata* (Knipfer *et al.*, 2019). We could not discern to what extent water stored in the xylem parenchyma had been reduced, but the close agreement between our microCT estimates, which included only fiber and vessel lumens, and our measurements of water storage suggests that storage in parenchyma is a minor fraction in this species.

Variation in capacitance was not associated with position in the tree or with organ diameter. Given that *C* did not change

across positions but water potential did, daily transpiration would result in more water being drawn per unit volume of xylem in distal stems compared to the shoot bole and roots. By virtue of its smaller size, any single distal stem has lower water-storage capacity compared to the bole, and hence such stems are at greater risk of conductive damage from negative water potentials caused by water loss. It therefore appeared that *C* was not being adjusted within tissues to buffer water potentials in the smaller shoots. Instead, damage from low water potentials in small stems is probably being prevented by development of greater resistance to cavitation through modification of other xylem traits such as xylem density (Jacobsen *et al.*, 2007), vessel density (Lens *et al.*, 2011; Jacobsen *et al.*, 2016), the intervessel dimensions of the pit aperture or pit membrane (Lens *et al.*, 2011; Jacobsen *et al.*, 2018), or the pore diameters within pit membranes (Jarbeau *et al.*, 1995; Wheeler *et al.*, 2005). However, these safeguards are not without limits and there is evidence of drought-induced dieback of branches in *Populus* species (Rood *et al.*, 2000).

### *Relationships between xylem functional traits*

Biomechanical functional traits and xylem density were negatively correlated with xylem water storage. Increased xylem strength and stiffness were correlated with a reduction of water storage capacity and a decline in water storage also correlated with increased xylem density. This indicates a trade-off, with the shoot xylem having a higher density and being stronger and stiffer but with limited per-volume water-storage capacity, and the root xylem having lower density and being weaker and less stiff but with greater per-volume water-storage capacity.

Xylem strength, stiffness, and density were correlated with each other, as has been reported in several previous studies (Woodrum *et al.*, 2003; Kern *et al.*, 2005; Jacobsen *et al.*, 2007; Chave *et al.*, 2009; Lachenbruch *et al.*, 2010). As xylem increases in density (dry mass per volume) it possesses a greater fraction of lignified wall (Niklas, 2000), less air volume, and the wood is often stiffer and stronger (Panshin and de Zeeuw, 1980). We found that the relationships between biomechanical traits and xylem density were weak to non-significant when examined only in the shoots, which was probably due to variations in other traits that can lead to divergence between strength and density, such as microfibril orientation (Panshin and de Zeeuw, 1980; Zhong *et al.*, 2002) or the lignin content of secondary walls (Voelker *et al.*, 2011). The biomechanical properties of secondary xylem can also be affected by different cell types and their arrangement and proportions, as illustrated by intraspecific studies that have found that xylem density is inversely related to MOE and MOR when stem samples have very divergent xylem arrangements due to varying numbers of nodes (Hepworth *et al.*, 2002; Bergman *et al.*, 2018).

Within the roots and across both shoots and roots, a reduction in *C* correlated with a lower water potential at the Phase 2-to-3 transition, $P_{2-3}$. This might reflect a general physical property of water loss from xylem. Assuming that the per-volume water-storage capacity is constant, less water released per unit pressure drop (i.e. lower *C*) would result in a lower water potential at the point of storage depletion. This pattern is consistent with interspecific studies that have shown that trees with lower *C* are found in drier regions and have lower minimum water potentials (Richards *et al.*, 2014), and that xylem with greater safety margins in terms of resistance to cavitation have lower *C* (Meinzer *et al.*, 2009).

### *Conclusions*

Intra-organismal studies compare tissue traits at different positions within the body in order to provide a better understanding of the functioning of the whole organism. These types of studies are also valuable in ascertaining the range of traits that plants are capable of producing in response to different conditions and treatments. We found that xylem functional traits changed according to the position along the main root-to-shoot axis and some traits showed ranges of several-fold trait variation within the plant body. Shoot xylem was biomechanically stronger and had lower water storage compared to roots. In roots, wider diameters at more proximal positions were associated with greater stiffness and strength, and increased xylem density. In shoots, narrow apical stems had increased xylem strength and stiffness relative to the basal bole. These differences were probably due to the differing hydraulic pressures and mechanical demands that occur at different positions within the tree. While some traits showed strong divergence between the root and shoot tissues with less variation within each of them (xylem density, water storage), others changed steadily and linearly along the root-to-shoot axis (stiffness, strength). Understanding how xylem functioning differs throughout tree bodies provides insight into how these large organisms develop, function, and respond to stresses.

## Supplementary data

The following supplementary data are available at *JXB* online.

Fig. S1. Relationships between position along the length of the shoots and roots and their diameters.

Fig. S2. Moisture release curves showing the relationships between cumulative water loss and water potential for all xylem samples.

Fig. S3. Water-storage traits in relation to organ length fraction and organ diameter of roots and shoots.

Fig. S4. Correlations between xylem water-storage traits and all other measured xylem traits.

## Acknowledgements

ABB thanks Isolde Francis for providing input as a member of the M.S. Thesis Committee. We thank Marta Percolla, Daniella Rodriguez, Jessica Valdovinos, Emily van Ryn, Martin D. Venturas, Jesica Gonzalez,

Lawrence Ignacio, Shana Carey, Hayden Toschi, and Angela Hill-Crim for assistance with field and laboratory measurements. We thank the reviewers and editor for their constructive and helpful comments and suggestions. Funding was provided to ABB by the CSUB Student Research Scholars program. This project was supported by the National Science Foundation (HRD-1547784 NSF to RBP and ALJ, IOS-1252232 to ALJ) and the Army Research Office of Department of Defense (68885-EV-REP, W911NF-16-1-0556 to RBP).

## Author contributions

ABB, RBP, and ALJ conceived the research plan; all authors assisted in data collection and initial analyses; ABB was responsible for final analyses, preparation of figures, and drafting the initial manuscript; ALJ revised the manuscript; all authors read, edited, and approved the final manuscript.

## Data availability

All data supporting the findings of this study are available within the paper and within its supplementary data published online.

## References

**Alder NN, Sperry JS, Pockman WT.** 1996. Root and stem xylem embolism, stomatal conductance, and leaf turgor in *Acer grandidentatum* populations along a soil moisture gradient. Oecologia **105**, 293–301.

**Alvarez-Clare S, Kitajima K.** 2007. Physical defence traits enhance seedling survival of neotropical tree species. Functional Ecology **21**, 1044–1054.

**Augspurger CK, Kelly CK.** 1984. Pathogen mortality of tropical tree seedlings: experimental studies of the effects of dispersal distance, seedling density, and light conditions. Oecologia **61**, 211–217.

**Baer AB.** 2018. Xylem functional traits at different tree positions within *Populus trichocarpa*. MS Biology Thesis, California State University, Bakersfield.

**Barnard DM, Meinzer FC, Lachenbruch B, McCulloh KA, Johnson DM, Woodruff DR.** 2011. Climate-related trends in sapwood biophysical properties in two conifers: avoidance of hydraulic dysfunction through coordinated adjustments in xylem efficiency, safety and capacitance. Plant, Cell & Environment **34**, 643–654.

**Bergman BA, Bobich EG, Davis SD, Utsumi Y, Ewers FW.** 2018. Dense but flexible wood – how leaf nodes impact xylem mechanics in *Juglans californica*. IAWA Journal **39**, 372–381.

**Borchert R, Pockman WT.** 2005. Water storage capacitance and xylem tension in isolated branches of temperate and tropical trees. Tree Physiology **25**, 457–466.

**Bouffier LA, Gartner BL, Domec JC.** 2003. Wood density and hydraulic properties of ponderosa pine from the Willamette valley vs. the Cascade mountains. Wood and Fiber Science **35**, 217–233.

**Butler DW, Gleason SM, Davidson I, Onoda Y, Westoby M.** 2012. Safety and streamlining of woody shoots in wind: an empirical study across 39 species in tropical Australia. New Phytologist **193**, 137–149.

**Chapotin SM, Razanameharizaka JH, Holbrook NM.** 2006. Water relations of baobab trees (*Adansonia* spp. L.) during the rainy season: does stem water buffer daily water deficits? Plant, Cell & Environment **29**, 1021–1032.

**Chave J, Coomes D, Jansen S, Lewis SL, Swenson NG, Zanne AE.** 2009. Towards a worldwide wood economics spectrum. Ecology Letters **12**, 351–366.

**Coutts MP.** 1986. Components of tree stability in Sitka spruce on peaty gley soil. Forestry **59**, 173–197.

**Domec JC, Gartner BL.** 2001. Cavitation and water storage capacity in bole xylem segments of mature and young Douglas-fir trees. Trees **15**, 204–214.

**Domec JC, Gartner BL.** 2002. Age- and position-related changes in hydraulic versus mechanical dysfunction of xylem: inferring the design criteria for Douglas-fir wood structure. Tree Physiology **22**, 91–104.

**Domec JC, Scholz FG, Bucci SJ, Meinzer FC, Goldstein G, Villalobos-Vega R.** 2006. Diurnal and seasonal variation in root xylem embolism in neotropical savanna woody species: impact on stomatal control of plant water status. Plant, Cell & Environment **29**, 26–35.

**Domec JC, Warren JM, Meinzer FC, Lachenbruch B.** 2009. Safety factors for xylem failure by implosion and air-seeding within roots, trunks and branches of young and old conifer trees. IAWA Journal **30**, 101–120.

**Hacke UG, Sperry JS, Pittermann J.** 2000. Drought experience and cavitation resistance in six shrubs from the Great Basin, Utah. Basic Applied Ecology **1**, 31–41.

**Hacke UG, Sperry JS, Pockman WT, Davis SD, McCulloh KA.** 2001. Trends in wood density and structure are linked to prevention of xylem implosion by negative pressure. Oecologia **126**, 457–461.

**Hepworth DG, Vincent JF, Stringer G, Jeronimidis G.** 2002. Variations in the morphology of wood structure can explain why hardwood species of similar density have very different resistances to impact and compressive loading. Philosophical Transactions of the Royal Society A, Mathematical, Physical, and Engineering Sciences **360**, 255–272.

**Holbrook NM.** 1995. Stem water storage. In: Gartner BL ed. Plant stems: physiology and functional morphology. San Diego, CA: Academic Press, 151–174

**Hölttä T, Cochard H, Nikinmaa E, Mencuccini M.** 2009. Capacitive effect of cavitation in xylem conduits: results from a dynamic model. Plant, Cell & Environment **32**, 10–21.

**Jacobsen AL, Agenbag L, Esler KJ, Pratt RB, Ewers FW, Davis SD.** 2007. Xylem density, biomechanics and anatomical traits correlate with water stress in 17 evergreen shrub species of the Mediterranean-type climate region of South Africa. Journal of Ecology **95**, 171–183.

**Jacobsen AL, Ewers FW, Pratt RB, Paddock WA, Davis SD.** 2005. Do xylem fibers affect vessel cavitation resistance? Plant Physiology **139**, 546–556.

**Jacobsen AL, Pratt RB, Venturas MD, Hacke UG.** 2019. Large volume vessels are vulnerable to water-stress-induced embolism in stems of poplar. IAWA Journal **40**, 4–22.

**Jacobsen AL, Tobin MF, Toschi HS, Percolla MI, Pratt RB.** 2016. Structural determinants of increased susceptibility to dehydration-induced cavitation in post-fire resprouting chaparral shrubs. Plant, Cell & Environment **39**, 2473–2485.

**Jacobsen AL, Valdovinos-Ayala J, Rodiguez-Zaccaro FD, Hill-Crim MA, Percolla MI, Venturas MD.** 2018. Intra-organismal variation in the structure of plant vascular transport tissues in poplar trees. Trees **32**, 1335–1346.

**Jansson S, Douglas CJ.** 2007. *Populus*: a model system for plant biology. Annual Review of Plant Biology **58**, 435–458.

**Jarbeau JA, Ewers FW, Davis SD.** 1995. The mechanism of water-stress-induced embolism in two species of chaparral shrubs. Plant, Cell and Environment **18**, 189–196.

**Johnson DM, Wortemann R, McCulloh KA, Jordan-Meille L, Ward E, Warren JM, Palmroth S, Domec JC.** 2016. A test of the hydraulic vulnerability segmentation hypothesis in angiosperm and conifer tree species. Tree Physiology **36**, 983–993.

**Jupa R, Plavcová L, Gloser V, Jansen S.** 2016. Linking xylem water storage with anatomical parameters in five temperate tree species. Tree Physiology **36**, 756–769.

**Kavanagh KL, Bond BJ, Aitken SN, Gartner BL, Knowe S.** 1999. Shoot and root vulnerability to xylem cavitation in four populations of Douglas-fir seedlings. Tree Physiology **19**, 31–37.

**Kern KA, Ewers FW, Telewski FW, Koehler L.** 2005. Mechanical perturbation affects conductivity, mechanical properties and aboveground biomass of hybrid poplars. Tree Physiology **25**, 1243–1251.

**King DA, Davies SJ, Supardi MN, Tan S.** 2005. Tree growth is related to light interception and wood density in two mixed dipterocarp forests of Malaysia. Functional Ecology **19**, 445–453.

**Knipfer T, Reyes C, Earles JM, Berry ZC, Johnson DM, Brodersen CR, McElrone AJ.** 2019. Spatiotemporal coupling of vessel cavitation and discharge of stored xylem water in a tree sapling. Plant Physiology **179**, 1658–1668.

**Lachenbruch B, Johnson GR, Downes GM, Evans R.** 2010. Relationships of density, microfibril angle, and sound velocity with stiffness and strength in mature wood of Douglas-fir. Canadian Journal of Forest Research **40**, 55–64.

**Lens F, Sperry JS, Christman MA, Choat B, Rabaey D, Jansen S.** 2011. Testing hypotheses that link wood anatomy to cavitation resistance and hydraulic conductivity in the genus *Acer*. New Phytologist **190**, 709–723.

**McCulloh KA, Johnson DM, Meinzer FC, Woodruff DR.** 2014. The dynamic pipeline: hydraulic capacitance and xylem hydraulic safety in four tall conifer species. Plant, Cell & Environment **37**, 1171–1183.

**McElrone AJ, Pockman WT, Martínez-Vilalta J, Jackson RB.** 2004. Variation in xylem structure and function in stems and roots of trees to 20 m depth. New Phytologist **163**, 507–517.

**Medeiros JS, Pockman WT.** 2014. Freezing regime and trade-offs with water transport efficiency generate variation in xylem structure across diploid populations of *Larrea* sp. (Zygophyllaceae). American Journal of Botany **101**, 598–607.

**Meinzer FC, Campanello PI, Domec JC, Genoveva Gatti M, Goldstein G, Villalobos-Vega R, Woodruff DR.** 2008. Constraints on physiological function associated with branch architecture and wood density in tropical forest trees. Tree Physiology **28**, 1609–1617.

**Meinzer FC, James SA, Goldstein G, Woodruff D.** 2003. Whole-tree water transport scales with sapwood capacitance in tropical forest canopy trees. Plant, Cell and Environment **26**, 1147–1155.

**Meinzer FC, Johnson DM, Lachenbruch B, McCulloh KA, Woodruff DR.** 2009. Xylem hydraulic safety margins in woody plants: coordination of stomatal control of xylem tension with hydraulic capacitance. Functional Ecology **23**, 922–930.

**Niklas KJ.** 1992. Plant biomechanics: an engineering approach to plant form and function. Chicago, IL: The University of Chicago Press.

**Niklas KJ.** 2000. The evolution of plant body plans—a biomechanical perspective. Annals of Botany **85**, 411–438.

**Olson ME.** 2012. The developmental renaissance in adaptationism. Trends in Ecology & Evolution **27**, 278–287.

**Olson ME, Anfodillo T, Gleason SM, McCulloh KA.** 2021. Tip-to-base xylem conduit widening as an adaptation: causes, consequences, and empirical priorities. New Phytologist **229**, 1877–1893.

**Olson ME, Rosell JA, Martínez-Pérez C, *et al.*** 2020. Xylem vessel-diameter–shoot-length scaling: ecological significance of porosity types and other traits. Ecological Monographs **90**, e01410.

**Panshin AJ, de Zeeuw C.** 1980. Textbook of wood technology. New York: McGraw-Hill.

**Plavcová L, Gallenmüller F, Morris H, Khatamirad M, Jansen S, Speck T.** 2019. Mechanical properties and structure–function trade-offs in secondary xylem of young roots and stems. Journal of Experimental Botany **70**, 3679–3691.

**Pratt RB, Black RA.** 2006. Do invasive trees have a hydraulic advantage over native trees? Biological Invasions **8**, 1331–1341.

**Pratt RB, Jacobsen AL.** 2017. Conflicting demands on angiosperm xylem: tradeoffs among storage, transport and biomechanics. Plant, Cell & Environment **40**, 897–913.

**Pratt RB, Jacobsen AL, Ewers FW, Davis SD.** 2007. Relationships among xylem transport, biomechanics and storage in stems and roots of nine Rhamnaceae species of the California chaparral. New Phytologist **174**, 787–798.

**Pratt RB, North GB, Jacobsen AL, Ewers FW, Davis SD.** 2010. Xylem root and shoot hydraulics is linked to life history type in chaparral seedlings. Functional Ecology **24**, 70–81.

**Putz FE, Coley PD, Lu K, Montalvo A, Aiello A.** 1983. Uprooting and snapping of trees: structural determinants and ecological consequences. Canadian Journal of Forest Research **13**, 1011–1020.

**Richards AE, Wright IJ, Lenz TI, Zanne AE.** 2014. Sapwood capacitance is greater in evergreen sclerophyll species growing in high compared to low-rainfall environments. Functional Ecology **28**, 734–744.

**Rood SB, Patiño S, Coombs K, Tyree MT.** 2000. Branch sacrifice: cavitation-associated drought adaptation of riparian cottonwoods. Trees **14**, 248–257.

**Rosell JA, Olson ME, Aguirre-Hernández R, Sánchez-Sesma FJ.** 2012. Ontogenetic modulation of branch size, shape, and biomechanics produces diversity across habitats in the *Bursera simaruba* clade of tropical trees. Evolution & Development **14**, 437–449.

**Sarmiento C, Patiño S, Paine CE, Beauchêne J, Thibaut A, Baraloto C.** 2011. Within-individual variation of trunk and branch xylem density in tropical trees. American Journal of Botany **98**, 140–149.

**Scholz FG, Bucci SJ, Goldstein G, Meinzer FC, Franco AC, Miralles-Wilhelm F.** 2007. Biophysical properties and function significance of stem water storage tissues in Neotropical savanna trees. Plant, Cell & Environment **30**, 236–248.

**Soriano D, Echeverría A, Anfodillo T, Rosell JA, Olson ME.** 2020. Hydraulic traits vary as the result of tip-to-base conduit widening in vascular plants. Journal of Experimental Botany **71**, 4232–4242.

**Spatz HC, Bruechert F.** 2000. Basic biomechanics of self-supporting plants: wind loads and gravitational loads on a Norway spruce tree. Forest Ecology and Management **135**, 33–44.

**Sperry JS, Adler FR, Campbell GS, Comstock JP.** 1998. Limitation of plant water use by rhizosphere and xylem conductance: results from a model. Plant, Cell & Environment **21**, 347–359.

**Sperry JS, Saliendra NZ.** 1994. Intra-and inter-plant variation in xylem cavitation in *Betula occidentalis*. Plant, Cell & Environment **17**, 1233–1241.

**Stokes A, Mattheck C.** 1996. Variation of wood strength in tree roots. Journal of Experimental Botany **47**, 693–699.

**Tyree MT, Ewers FW.** 1991. The hydraulic architecture of trees and other woody plants. New Phytologist **119**, 345–360.

**Tyree MT, Yang S.** 1990. Water-storage capacity of *Thuja*, *Tsuga* and *Acer* stems measured by dehydration isotherms: The contribution of capillary water and cavitation. Planta **182**, 420–426.

**Tyree MT, Zimmermann MH.** 2002. Xylem structure and the ascent of sap, 2nd edn. Berlin: Springer-Verlag.

**Utsumi Y, Bobich EG, Ewers FW.** 2010. Photosynthetic, hydraulic and biomechanical responses of *Juglans californica* shoots to wildfire. Oecologia **164**, 331–338.

**van Gelder HA, Poorter L, Sterck FJ.** 2006. Wood mechanics, allometry, and life-history variation in a tropical rain forest tree community. New Phytologist **171**, 367–378.

**Venturas MD, Pratt RB, Jacobsen AL, Castro V, Fickle JC, Hacke UG.** 2019. Direct comparison of four methods to construct xylem vulnerability curves: differences among techniques are linked to vessel network characteristics. Plant, Cell & Environment **42**, 2422–2436.

**Venturas MD, Sperry JS, Hacke UG.** 2017. Plant xylem hydraulics: what we understand, current research, and future challenges. Journal of Integrative Plant Biology **59**, 356–389.

**Voelker SL, Lachenbruch B, Meinzer FC, Strauss SH.** 2011. Reduced wood stiffness and strength, and altered stem form, in young antisense *4CL* transgenic poplars with reduced lignin contents. New Phytologist **189**, 1096–1109.

**Wheeler JK, Sperry JS, Hacke UG, Hoang N.** 2005. Inter-vessel pitting and cavitation in woody Rosaceae and other vesselled plants: a basis for a safety versus efficiency trade-off in xylem transport. Plant, Cell & Environment **28**, 800–812.

**Woodrum CL, Ewers FW, Telewski FW.** 2003. Hydraulic, biomechanical, and anatomical interactions of xylem from five species of *Acer* (Aceraceae). American Journal of Botany **90**, 693–699.

**Zhong R, Burk DH, Morrison WH III, Ye ZH.** 2002. A kinesin-like protein is essential for oriented deposition of cellulose microfibrils and cell wall strength. The Plant Cell **14**, 3101–3117.

**Ziemińska K, Rosa E, Gleason SM, Holbrook NM.** 2020. Wood day capacitance is related to water content, wood density, and anatomy across 30 temperate tree species. Plant, Cell & Environment **43**, 3048–3067.